Decoherence dynamics of a charge qubit coupled to the noise bath*

Yang Qin-Ying(杨芹英)[a], Liang Bao-Long(梁宝龙)[a], and Wang Ji-Suo(王继锁)[a,b]†

[a] School of Physics Science and Information Engineering, Liaocheng University, Liaocheng 252059, China
[b] College of Physics and Engineering, Qufu Normal University, Qufu 273165, China

(Received 29 November 2012; revised manuscript received 13 February 2013)

By virtue of the canonical quantization method, we present a quantization scheme for a charge qubit based on the superconducting quantum interference device (SQUID), taking the self-inductance of the loop into account. Under reasonable short-time approximation, we study the effect of decoherence in the ohmic case by employing the response function and the norm. It is confirmed that the decoherence time, which depends on the parameters of the circuit components, the coupling strength, and the temperature, can be as low as several picoseconds, so there is enough time to record the information.

Keywords: charge qubit, decoherence, response function, norm

PACS: 03.65.Yz, 68.65.–k, 03.65.–w **DOI:** 10.1088/1674-1056/22/7/070301

1. Introduction

Due to their easy integration in the forming of large-scale circuits and scalable quantum information processing, nanoscale solid-state qubits, especially superconducting qubits based on Josephson junctions, are considered to be leading candidates in this field.[1–4] A basic type of these qubits is the Josephson junction charge qubit (JJCQB), and the simplest model of the JJCQB is proposed. One of its significant advantages is direct operation controlled by external voltage sources.[5] In the vicinity of a degeneracy voltage point, the proposed system is reduced effectively to a two-state quantum system, which is used as the local states $|0\rangle$ and $|1\rangle$.[6] However, such an isolated model is only an ideal case since any practical models are always affected more or less by their environment. Decoherence (i.e., the destruction of quantum coherence induced usually by the interaction between qubits and their environment) may be the primary obstacle for the qubit to be taken as the cell of a quantum computer. Hence, it is important to explore the roles of various dominant decoherence origins and mechanisms. Decoherence has recently been widely studied both theoretically and experimentally.[7–11] The common methods used in these studies include the Born–Markov approximation, the quasiadiabatic propagator path integral method, and the short-time approximation. Increasing attention has been paid to the decoherence dynamics of two-state systems in the presence of the noise bath for promising quantum computations. It would therefore be interesting to describe such a system and explore its mechanism. In this work, we take advantage of some reasonable approximations to investigate decoherence dynamics, by reference to a concrete model, i.e., a charge qubit based on superconducting quantum interference devices (SQUIDs).

This paper is structured as follows. In Section 2, we begin with the introduced model and a brief general formula derivation by means of some reasonable approximation in order to obtain an analytic expression of the system Hamiltonian. Then, we explain the reason why the system can be regarded as a two-state one. In Section 3, we try to analyze the decoherence time of the system mainly using two methods: response function and norm. The last section provides the conclusion.

2. The model and electric circuit quantization

The mesoscopic electric circuit of the JJCQB based on SQUID is shown in Fig. 1. It consists of a coupling capacitance C and a small superconducting island, labeled by the dashed line, which connects two tunnel junctions with capacitance $C_{\rm j}$ and Josephson coupling energy $E_{\rm j}$ to a superconducting electrode. A control gate voltage $V_{\rm g}$ is coupled via a gate capacitance $C_{\rm g}$ to the system. For a single Josephson junction,

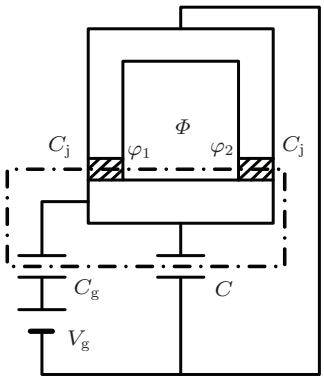


Fig. 1. A charge qubit with tunable coupling via the gate voltage and the external magnetic flux.

*Project supported by the National Natural Science Foundation of China (Grant Nos. 11147009 and 11244005) and the Natural Science Foundation of Shandong Province, China (Grant Nos. ZR2010AQ027 and ZR2012AM004).

†Corresponding author. E-mail: jswang@lcu.edu.cn

© 2013 Chinese Physical Society and IOP Publishing Ltd

the two characteristic Josephson equations are given by

$$I_{\rm j} = I_{\rm c}\sin\varphi_{\rm j}, \quad \dot{\varphi}_{\rm j} = \frac{2e}{\hbar}u_{\rm j}, \tag{1}$$

where $\varphi_{\rm j}$ is the phase difference between two electrode orders across the junction, and $I_{\rm c} = 2eE_{\rm j}/\hbar$ is the critical current.

We now focus on the classical Hamiltonian of the system via the principle of canonical quantization. Regarding φ_{ji} $(i = 1,2)$ as the generalized coordinates, the Lagrangian of the system[12] is

$$\begin{aligned}\mathscr{L} &= \mathscr{T} - \mathscr{V} = \left[\frac{1}{2}\left(\frac{\hbar}{2e}\right)^2 C_\Sigma\dot{\varphi}^2 + n_{\rm g}\hbar\dot{\varphi} + \frac{2e^2n_{\rm g}^2}{C_{\rm g}}\right] \\ &\quad - 2E_{\rm j}\left[1 - \cos\left(\frac{e}{\hbar}\Phi\right)\cos\varphi\right],\end{aligned} \tag{2}$$

where $C_\Sigma = 2C_{\rm j} + C + C_{\rm g}$, $\varphi = (\varphi_1 + \varphi_2)/2$, and $n_{\rm g} = C_{\rm g}V_{\rm g}/(2e)$ are, respectively, the equivalent total capacitance of the system, the mean phase, and the gate charge number, which plays the role of a control parameter. The magnetic flux Φ through the SQUID loop, which must be the integer multiple of the magnetic flux on the magnetic flux quantum Φ_0 ($\Phi_0 = 2.0678\times10^{-15}$ W), includes the external classical magnetic flux Φ_x. Using Eq. (2), we can obtain the generalized momentum $p_{\rm j}$ conjugated to $\dot{\varphi}$ as

$$p_{\rm j} = \frac{\partial\mathscr{L}}{\partial\dot{\varphi}} = \frac{1}{2}\left(\frac{\hbar}{2e}\right)^2 C_\Sigma 2\dot{\varphi} + n_{\rm g}\hbar = n\hbar, \tag{3}$$

where n is the excess number of Cooper pairs tunneling across the island. Apparently, the generalized momentum $p_{\rm j}$ is proportional to n. Note that the number n follows the relation $\sum_{i=1}^{2} C_{\rm j}u_{ji} - 2ne = -Cu_{\rm c} - C_{\rm g}u_{\rm g}$, which is based on the principle of continuity of the electric current at the nodes of the circuit. From Eqs. (2) and (3), the classical Hamiltonian can be written as

$$H = p_{\rm j}\dot{\varphi}_{\rm j} - \mathscr{L} = 4E_{\rm c}(n - n_{\rm g})^2 - 2E_{\rm j}\cos\left(\frac{e}{\hbar}\Phi\right)\cos\varphi, \tag{4}$$

where the single-electron charging energy $E_{\rm c} = e^2/(2C_\Sigma)$ depends on the total capacitance of the island. Here, we have neglected some constant terms which only cause the superconducting energy level to shift. According to Dirac's standard canonical quantization principle, to endow the quantization condition, i.e., the commutation relation $[n,\varphi] = -{\rm i}$, the Hamiltonian operator can be expressed as

$$\hat{H} = 4E_{\rm c}(\hat{n} - n_{\rm g})^2 - 2E_{\rm j}\cos(e\hat{\Phi}/\hbar)\cos\hat{\varphi}. \tag{5}$$

In addition, the self-inductance usually needs to be included for the SQUID single-charge qubit and the circulating current satisfies[13]

$$\begin{aligned}\hat{I} &= I_{\rm c}(\sin\hat{\varphi}_2 - \sin\hat{\varphi}_1) = 2I_{\rm c}\cos\hat{\varphi}\sin\left(\frac{e}{\hbar}\Phi_x + \frac{e}{\hbar}L\hat{I}\right) \\ &= 2I_{\rm c}\cos\hat{\varphi}\left[\sin\left(\frac{e}{\hbar}\Phi_x\right)\sum_{m=0}^{\infty}\frac{(-1)^m(eL\hat{I}/\hbar)^{2m}}{(2m)!}\right. \\ &\quad \left. + \cos\left(\frac{e}{\hbar}\Phi_x\right)\sum_{m=1}^{\infty}\frac{(-1)^{m-1}(eL\hat{I}/\hbar)^{2m-1}}{(2m-1)!}\right],\end{aligned} \tag{6}$$

where L is the self-inductance coefficient for the SQUID loop. As $\hat{I}$ is a continuous function of $\cos\varphi$, it can be expanded into the Taylor series as follows: $\hat{I} = 2I_{\rm c}\cos\hat{\varphi}\sum_{m=1}^{\infty} a_m\cos^{m-1}\hat{\varphi}$. Comparing the coefficients of $\cos^m\hat{\varphi}$ on both sides of Eq. (6), we have

$$\begin{aligned}a_1 &= \sin\left(\frac{e}{\hbar}\Phi_x\right), \quad a_2 = \frac{1}{2}\left(\frac{2eI_{\rm c}L}{\hbar}\right)\sin\left(\frac{e}{\hbar}\Phi_x\right), \\ a_3 &= \left(\frac{2eI_{\rm c}L}{\hbar}\right)^2\sin\left(\frac{e}{\hbar}\Phi_x\right)\left[1 - \frac{3}{2}\sin^2\left(\frac{e}{\hbar}\Phi_x\right)\right], \\ a_4 &= \frac{1}{2}\left(\frac{2eI_{\rm c}L}{\hbar}\right)^3\sin\left(\frac{2e}{\hbar}\Phi_x\right)\left[1 - \frac{8}{3}\sin^2\left(\frac{e}{\hbar}\Phi_x\right)\right], \\ &\vdots\end{aligned} \tag{7}$$

Similarly, because $E_{\rm J}(\hat{\Phi}) = 2E_{\rm j}[\cos(e\Phi_x/\hbar + eL\hat{I}/\hbar)]$ can also be expanded into the Taylor series about $\hat{I}$, $E_{\rm J}(\hat{\Phi}) = 2E_{\rm j}\sum_{m=1}^{\infty} b_m\cos^m\hat{\varphi}$, we have

$$\begin{aligned}b_0 &= \cos\left(\frac{e}{\hbar}\Phi_x\right), \quad b_1 = -\left(\frac{2eI_{\rm c}L}{\hbar}\right)\sin^2\left(\frac{e}{\hbar}\Phi_x\right), \\ b_2 &= -\frac{3}{2}\left(\frac{2eI_{\rm c}L}{\hbar}\right)^2\cos\left(\frac{e}{\hbar}\Phi_x\right)\sin^2\left(\frac{e}{\hbar}\Phi_x\right), \\ b_3 &= -2\left(\frac{2eI_{\rm c}L}{\hbar}\right)^3\sin^2\left(\frac{e}{\hbar}\Phi_x\right)\left[1 - \frac{4}{3}\sin^2\left(\frac{e}{\hbar}\Phi_x\right)\right], \\ &\vdots\end{aligned} \tag{8}$$

For the model above, $L \sim 1$nH we suggested, which can induce an interaction of adequate strength, will suffice. Typically, $2eI_{\rm c}L/\hbar \sim 10^{-3}$ can be considered as a desirable approximation. In light of the above comprehensive consideration, the Hamiltonian operator can be rewritten as

$$\hat{H} = 4E_{\rm c}(\hat{n} - n_{\rm g})^2 - 2E_{\rm j}\sum_{m=0}^{3} b_m\cos^{m+1}\hat{\varphi}. \tag{9}$$

Here, we shall review the quantum dynamics in the regime of $E_{\rm c} \gg E_{\rm j}$, where the charge on the superconducting islands is the appropriate quantum degree of freedom. In this instance, a convenient basis formed by the charge states can be parameterized by the number of Cooper pairs n on the island. Thus, equation (9) can be rewritten as

$$\begin{aligned}\hat{H} &= \sum_n 4E_{\rm c}(\hat{n} - n_{\rm g})^2|n\rangle\langle n| \\ &\quad - 2E_{\rm j}\sum_{m=0}^{3} b_m\left[\frac{1}{2}(|n\rangle\langle n+1| + |n+1\rangle\langle n|)\right]^{m+1}.\end{aligned} \tag{10}$$

If n_g is approximately half-integer, and the charging energies of the two adjacent states are close to each other, then Josephson tunneling will mix them strongly. When the temperature T is low enough and the gate-voltage range is near a degeneracy point where only the two states $|n=0\rangle$ and $|n=1\rangle$ play an important role, all the other charge states with a much higher energy can be neglected. In this case, the system is reduced to a two-state quantum system. Then, by virtue of the Pauli operators, we can express the Hamiltonian as

$$\hat{H}_S = -\frac{1}{2}B_z\hat{\sigma}_z - \frac{1}{2}B_x\hat{\sigma}_x, \tag{11}$$

where $B_z = 4E_c(1-2n_g)$ corresponds to the z component of the magnetic field controlled by the gate voltage, and $B_x = 2E_j(b_0 + b_2/4)$ corresponds to the x component of the effective magnetic field in spin notation.

The system described by Eq. (11) is an isolated one. In general, it is impossible to have almost all real-life systems completely isolated from their environment. The interaction between them may unavoidably cause qubit decoherence. In the following section, we will use the response function and the norm[14,15] to study this problem.

3. Decoherence of the charge qubit

Neglecting the effect of any residual terms coupling to $\hat{\sigma}_x$ and $\hat{\sigma}_y$ (because they have only nondiagonal matrix elements in the $\hat{\sigma}_z$ representation), the influence of the thermal reservoir can be reflected entirely by the term coupled only to $\hat{\sigma}_z$.[16] Generally, this can be treated as a set of harmonic oscillators. By employing the spin-boson model,[17,18] we may describe the above two-state system coupled to such a bath. In the "spin" $\hat{\sigma}_z$ representation of a qubit, the total Hamiltonian of the system can be written as

$$\begin{aligned}\hat{H} &= \hat{H}_S + \hat{H}_I + \hat{H}_R \\ &= -\frac{1}{2}B_z\hat{\sigma}_z - \frac{1}{2}B_x\hat{\sigma}_x + \hat{\sigma}_z\sum_i[c_i(\hat{a}_i^\dagger + \hat{a}_i)] \\ &\quad + \sum_i(\hbar\omega_i\hat{a}_i^\dagger\hat{a}_i),\end{aligned} \tag{12}$$

where $\hat{H}_I = \hat{\sigma}_z\sum_i[c_i(\hat{a}_i^\dagger + \hat{a}_i)]$ and $H_R = \sum_i(\hbar\omega_i\hat{a}_i^\dagger\hat{a}_i)$ are, respectively, the interaction part and the thermal reservoir of the Hamiltonian, parameter c_i the coupling constant, and $\hat{a}_i^\dagger(\hat{a}_i)$ is the creation (annihilation) operator of the i-th thermal mode.

3.1. Response function

It has been shown that comprehensive information about the effect of the thermal reservoir is encapsulated in the spectral function $J(\omega)$, because any problem can be taken over the initial states of the environment and a sum over the final states in a thermal equilibrium statistical average.[19] The spectral density of the thermal reservoir is given by

$$\begin{aligned}J(\omega) &= \frac{\pi}{2}\sum_i[c_i^2\delta(\omega-\omega_i)] \\ &= \frac{\pi}{2}\hbar\alpha\omega\left(\frac{\omega}{\omega_c}\right)^{s-1}\exp\left(-\frac{\omega}{\omega_c}\right),\end{aligned} \tag{13}$$

where ω_c is the high-frequency cutoff of the model. As ω tends to be infinite, $J(\omega)$ tends to be zero and is the cutoff at the higher frequency end; as ω tends to be zero, $J(\omega)$ tends to be a constant. The $s>1$ case is usually called the "super-ohmic" case; the $s=1$ case is "ohmic"; the $0<s<1$ case is "sub-ohmic"; and the $s\leq 0$ case is pathological. The α parameter is the dimensionless strength of the dissipation describing the coupling between the two-state system and the environment. In this paper, we focus on the weak damping, $\alpha \ll 1$, because only this regime plays a major role in quantum state engineering. Simultaneously, we mainly concentrate on the decoherence of the ohmic case, for which the situation, i.e., the zero bias case $B_z\hat{\sigma}_z = 0$, is relatively simple, corresponding to the spectral density of the form

$$J(\omega) = \frac{\pi}{2}\hbar\alpha\omega\exp\left(-\frac{\omega}{\omega_c}\right). \tag{14}$$

Note that a promising qubit should exhibit prolonged coherent oscillations while integrated in large structures. Therefore, it is necessary to investigate the decoherence dynamics. The QUAPI solution has been proposed to deal with this problem.[20] Using such a method, the influence function can be expressed with a product of terms corresponding to different point intervals of discrete path integral expressions. Then, the length of the memory time can be obtained from the bath response function[21]

$$\begin{aligned}L(t) &= \frac{1}{\pi}\int_0^{+\infty}J(\omega)\left[\coth\left(\frac{\beta\hbar\omega}{2}\right)\right. \\ &\quad \left.\times\cos(\omega t) - \mathrm{i}\sin(\omega t)\right]\mathrm{d}\omega,\end{aligned} \tag{15}$$

where $\beta = 1/(k_B T)$, k_B is the Boltzmann constant, and T is the temperature of the system. We can confirm from Eq. (15) that $L(t)$ satisfies the relation $L^*(t) = L(-t)$, and the imaginary part $\mathrm{Im}[L(t)]$ of the response function $L(t)$ has nothing to do with the temperature T, while the real part $\mathrm{Re}[L(t)]$ depends on the coefficient α as well as the temperature T. It is shown that the dynamics of the reduced density matrix are Markovian when the real and imaginary parts of $L(t)$ behave as the function $\delta(t)$ and its derivative $\delta'(t)$. Otherwise, they will be non-Markovian.

With the help of detailed numerical analysis and drafting, we now turn to the memory of the temporal evolution. The mesoscopic parameters are set to be $C = C_g = 10^{-16}$ F, $C_J = 10^{-15}$ F,[22] $\omega_c = 5\ \mathrm{ps}^{-1}$, and $T = 30$ mK[23] (see Fig. 2).

Note that the response function drops off rapidly as the time evolves until $L \to 0$, i.e., the influence of the environment quickly becomes weak with the increase in the "interaction distance". The broader the $\mathrm{Im}[L(t)]$ and $\mathrm{Re}[L(t)]$ are, the longer the memory time will be. From Figs. 2(a) and 2(b), we can obtain that the length of the memory time is about 3 ps, which shows that the influence of the bath results in a shorter decoherence time than the experimental value of 1 ns.[24,25]

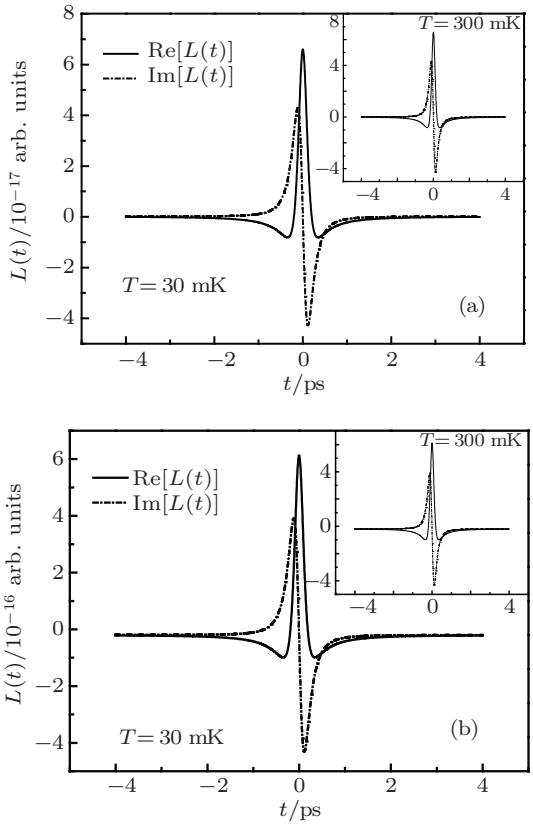


Fig. 2. The variation tendency of the bath response function $L(t)$ for the spectral function $J(\omega)$ of the system for the ohmic case. (a) $\alpha = 0.5 \times 10^{-7}$, (b) $\alpha = 0.5 \times 10^{-6}$. The solid and dashed lines denote the real part $\mathrm{Re}[L(t)]$ and the imaginary part $\mathrm{Im}[L(t)]$ of $L(t)$, respectively. The insets show $\mathrm{Re}[L(t)]$ and $\mathrm{Im}[L(t)]$ versus time t for $T = 300$ mK.

In addition, the length of the memory time has little difference for different temperatures. It is shown that the temperature T plays a subordinate role in the decoherence of the cryogenic superconducting world, while the strength of the dissipation α dominates over T since it has a greater influence on the strength of decoherence by some orders of magnitude. For instance, different values of α can yield a remarkable amplitude variation in $L(t)$ from the scale of the coordinate axis, as the above figures show. As a matter of fact, the time of the elementary quantum gate operation is much shorter than that of the thermal relaxation, yet the influence of the environment-induced decoherence must be kept below a certain boundary value during short-time intervals in order to enable fault-tolerant quantum error correction.[26] For comparison, based on the short-time approximation, we shall use the norm to discuss the decoherence of this system from another perspective in the next section.

3.2. Norm

It has been demonstrated that the decoherence can be reflected by the evolution of the off-diagonal elements of its reduced density matrix. Actually, the initial state of the system is supposed to be

$$R(0) = \rho(0) \otimes \rho_{\mathrm{R}}(0), \tag{16}$$

where $\rho(0)$ is the initial state of the qubit, and

$$\rho_{\mathrm{R}}(0) = \exp(-\beta\hbar\omega_i \hat{a}_i^{\dagger}\hat{a}_i)/\mathrm{Tr}_{\mathrm{R}}[\exp(-\beta\hbar\omega_i \hat{a}_i^{\dagger}\hat{a}_i)]$$

is the initial state of the bath. Usually, the reduced density matrix of the quantum system with the environment traced out is estimated using some approximation schemes.[27] The evolution of the reduced density matrix elements of the system, with the short-time approximation[28,29] taken into account, can be expressed as

$$\begin{aligned}\rho_{\mu\nu}(t) \;=\; & \mathrm{Tr}_{\mathrm{R}}\langle\mu|\exp(-\mathrm{i}\hat{H}_{\mathrm{S}}t/2\hbar)\exp[-\mathrm{i}(\hat{H}_{\mathrm{I}}+\hat{H}_{\mathrm{R}})t/\hbar] \\ & \times \exp(-\mathrm{i}\hat{H}_{\mathrm{S}}t/2\hbar)R(0)\exp(\mathrm{i}\hat{H}_{\mathrm{S}}t/2\hbar) \\ & \times \exp[\mathrm{i}(\hat{H}_{\mathrm{I}}+\hat{H}_{\mathrm{R}})t/\hbar]\exp(\mathrm{i}\hat{H}_{\mathrm{S}}t/2\hbar)|\nu\rangle, \\ & (\mu,\nu = 0,1).\end{aligned} \tag{17}$$

We can use the deviation operator $\sigma(t) = \rho(t) - \rho^{(i)}(t)$ to quantify the effect of the interaction,[30] where $\rho(t)$ and $\rho^{(i)}(t) = \exp(-\mathrm{i}\hat{H}_{\mathrm{S}}t/\hbar)\rho(0)\exp(\mathrm{i}\hat{H}_{\mathrm{S}}t/\hbar)$ correspond to the density matrix of the real evolution (with interaction) and the ideal evolution (without interaction) of the investigated system, respectively. To describe the decoherence of the short-time evolution, we can use the deviation operator norm

$$\|\sigma\|_{\lambda} = \sup_{\varphi\neq 0}(\langle\varphi|\sigma|\varphi\rangle/\langle\varphi|\varphi\rangle)^{1/2}. \tag{18}$$

Clearly, $\|\sigma\|_{\lambda}$ is a function of time, and depends on the initial density operator $\rho(0)$. For the two-state system, $\|\sigma\|_{\lambda} = (|\sigma_{10}|^2 + |\sigma_{11}|^2)^{1/2}$. In general, the influence of the bath can be better quantified by the maximal norm

$$D(t) = \sup_{\rho(0)}(\|\sigma(t,\rho(0))\|_{\lambda}). \tag{19}$$

From Eq. (19), we can see that $D(t)$ is confined to a fairly small range, $0 \le D(t) \le 1$. Substituting Eq. (17) into Eq. (19) yields

$$\sigma_{10}(t) \;=\; \frac{1}{2}\rho_{10}(0)[1-\mathrm{e}^{-B^2(t)}](1-\mathrm{e}^{-\mathrm{i}B_x t/\hbar}), \tag{20}$$

$$\sigma_{11}(t) \;=\; \frac{1}{2}[1-\mathrm{e}^{-B^2(t)}][\rho_{00}(0)-\rho_{11}(0)], \tag{21}$$

$$\begin{aligned}\|\sigma(t)\|_{\lambda} \;=\; & \frac{1}{2}[1-\mathrm{e}^{-B^2(t)}]\{[\rho_{00}(0)-\rho_{11}(0)]^2 \\ & +4|\rho_{10}(0)|^2\sin^2(E_{\mathrm{J}}(\Phi_x)t/2\hbar)\}^{1/2},\end{aligned} \tag{22}$$

where

$$B^2(t) = 8\int_0^{+\infty}(\alpha/2\omega)\exp(-\omega/\omega_c)\sin^2(\omega t/2) \times \coth(\beta\hbar\omega/2)\,\mathrm{d}\omega.$$

It is proved that the norm is also appropriate for practical computation and measuring the characteristics of the initial decoherence based on the short-time approximation. The evolution of the norm can be deduced from the parameters of the system as long as the initial state is given. In order to numerically analyze the decoherence of the system, we can plot $\|\sigma(t)\|_\lambda - t$ (as shown in Figs. 3(a)–3(c)). The parameters we used were $T = 30$ mK, $\omega_c = 5$ ps^{-1}, $E_J \sim 100$ mK (the same as those in Fig. 2), and $\Phi_x = \Phi_0$.[31]

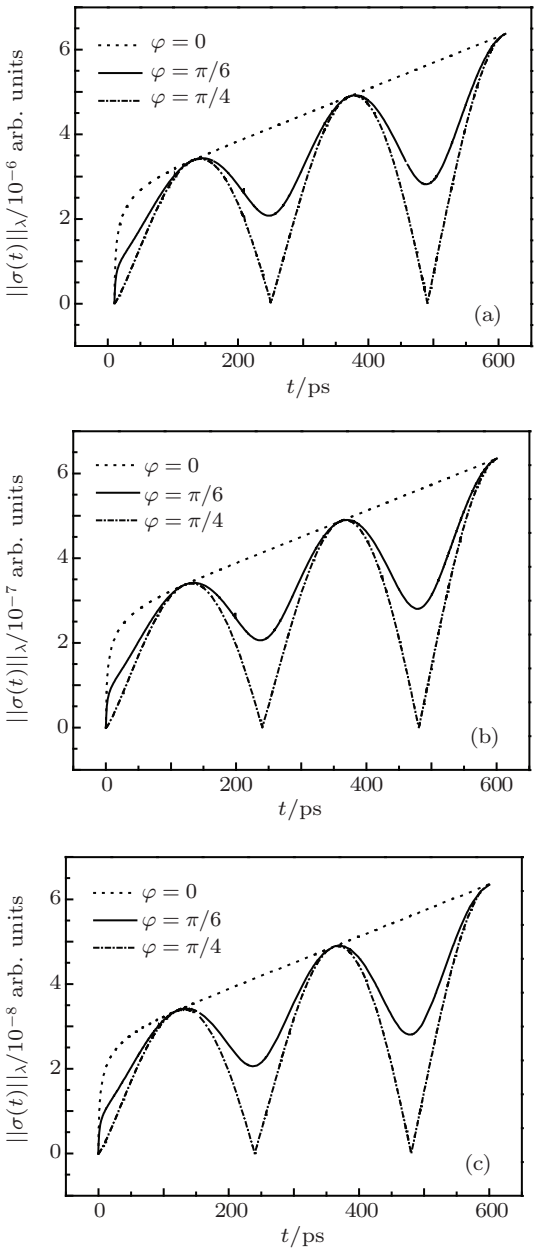


Fig. 3. The deviation norm for a two-state system interacting with the ohmic case of modes in the short-time approximation. (a) $\alpha = 0.5\times10^{-6}$, (b) $\alpha = 0.5\times10^{-7}$, and (c) $\alpha = 0.5\times10^{-8}$. The dotted, solid, and dashed lines, respectively, correspond to three initial states, which are $(1, 0)^{\mathrm{T}}$, $(\sqrt{3}/2, 1/2)^{\mathrm{T}}$ and $(\sqrt{2}/2, \sqrt{2}/2)^{\mathrm{T}}$.

The oscillatory curves demonstrate the $\|\sigma(t)\|_\lambda$ norms for the three different initial states $|\varphi\rangle_0 = (\cos\varphi_0, \sin\varphi_0)^{\mathrm{T}}$, which are, respectively, $\varphi_0 = 0$, $\varphi_0 = \pi/6$, and $\varphi_0 = \pi/4$. It is shown that when $\varphi_0 = 0$, $\|\sigma(t)\|_\lambda$ is the maximum, and the same with $D(t) = [1 - \mathrm{e}^{B^2(t)}]/2$. In addition, $D(t)$ increases with time t and $D(\infty) = 1/2$ (see the dotted line in Fig. 3). The latter two cases oscillate with time periodically (see the solid and dashed lines in Fig. 3). Comparing Figs. 3(a)–3(c), we find that $\|\sigma(t)\|_\lambda$ in common increases from zero with time due to the decoherence. For different values of the dimensionless strength of the dissipation α, $\|\sigma(t)\|_\lambda$ varies greatly, which means that the decoherence increases with increasing α. However, the profiles keep similar shapes and are independent of the value of α. Generally, $D \leq 10^{-4}$ is regarded as low decoherence. From Figs. 3(a)–3(c), we can estimate that the decoherence time of the two-state system is about 150 ps, which is longer than the characteristic time of the gate operation (i.e., 12.7 ps[32]), and those obtained on the response function. In a word, the experimental results and theoretical results both indicate that this system has enough decoherence time, and thus the charge qubit is used for quantum computation and manipulation.

4. Conclusions

In conclusion, we studied a charge qubit based on SQUID by coupling the symmetric feature of a single JJCQB to a noise bath, and looked at the quantization scheme of the mesoscopic electric circuit. Predictions of the model are reasonable since they are based on some approximation methods. We first employ the response function to reflect the length of the memory time, and then the norm to demonstrate the short-time decoherence of the ohmic case. It is demonstrated that the decoherence time, which is in the order of picoseconds, mainly depends on the coupling strength, temperature, and initial states. In addition, the strength of the dissipation α has nothing to do with the curve shape, and only keeps in touch with the strength of the decoherence. Therefore, by tuning some reasonable parameters, we can appropriately suppress the decoherence of the superconducting qubit. In a word, the charge qubit is considered as a promising candidate for quantum information processing.

References

[1] Josephson B D 1964 *Rev. Mod. Phys.* **36** 216
[2] Vourdas A 1996 *J. Mod. Opt.* **43** 2105
[3] Brandes T 2005 *Phys. Rep.* **408** 315
[4] Ji Y H and Liu Y M 2013 *Chin. Phys. B* **22** 020305
[5] Shirman A, Schon G and Hermon Z 1997 *Phys. Rev. Lett.* **79** 2371
[6] Korotkov A N 1999 *Phys. Rev. B* **60** 5737
[7] Petta J R, Johnson A C, Marcus C M, Hanson M P and Gossard A C 2004 *Phys. Rev. Lett.* **93** 186802

[8] Fedichkin L, Yanchenko M and Valiev K A 2000 *Nanotechnology.* **11** 387

[9] Gardelis S, Smith C G, Cooper J, Ritchie D A, Linfield E H, Jin Y and Pepper M 2003 *Phys. Rev. B* **67** 073302

[10] Yan Y Y, Qin L G and Tian L J 2012 *Chin. Phys. B* **21** 100304

[11] Zhang X X and Li F L 2011 *Chin. Phys. B* **20** 110302

[12] Goldstein H 1980 *Classical Mechanics* (2nd edn.) (Addision-Wesley Publishing Company)

[13] Liang B L, Wang J S, Fan H Y and Meng X G 2008 *Chin. Phys. Lett.* **25** 3753

[14] Privman V and Stat J 2003 *Phys.* **110** 957

[15] Fedichin L and Fedorov A 2004 *Phys. Rev. A* **69** 032311

[16] Leggett A J, Chakravarty S, Dorsey A T, Fisher M P A, Garg A and Zwerger W 1987 *Rev. Mod. Phys.* **59** 1

[17] Morozov V G, Mathey S and Röpke G 2012 *Phys. Rev. A* **85** 022101

[18] Weiss U 1999 *Quantum Dissipative Systems* (2nd edn.) (Singapore: World Scientific)

[19] Huelga S F and Plenio M B 2007 *Phys. Rev. Lett.* **98** 170601

[20] Liang X T 2005 *Phys. Rev. B* **72** 245328

[21] Markri N and Makarov D E 1995 *J. Chem. Phys.* **102** 4600

[22] Liang B L, Wang J S, Meng X G and Su J 2010 *Chin. Phys. B* **19** 010315

[23] Liang X T, Zhang W M and Zhuo Y Zh 2010 *Phys. Rev. E* **81** 011906

[24] Hayashi T, Fujisawa T, Cheong H D, Jeong Y H and Hirayama Y 2003 *Phys. Rev. Lett.* **91** 226804

[25] Petta J R, Johnson A C, Marcus C M, Hanson M P and Gossard A C 2004 *Phys. Rev. Lett.* **93** 186802

[26] Steane A M 1996 *Phys. Rev. A* **54** 47411

[27] Zurek W H 2003 *Rev. Mod. Phys.* **75** 715

[28] Gray S K and Verosky J M 1993 *J. Chem. Phys.* **99** 8680

[29] Blanes S and Moan P C 2000 *Phys. Lett. A* **265** 35

[30] Fedichkin L, Fedorov A and Privman V 2003 *Proc. SPIE.* **5105** 243

[31] Makhlin Y, Schon G and Shnirman A 2001 *Rev. Mod. Phys.* **73** 357

[32] Liang X T and Xiong Y J 2004 *Phys. Lett. A* **332** 8